

Supporting Information for
Environmental Science and Technology

**Kinetic Isotope Effects of the Enzymatic Transformation of
 γ -Hexachlorocyclohexane by Lindane Dehydrochlorinase
Variants LinA1 and LinA2**

Iris E. Schilling^{1,2}, Ramon Hess², Jakov Bolotin¹, Rup Lal³,
Thomas B. Hofstetter^{1,2} and Hans-Peter E. Kohler^{*,1,2}

¹Eawag, Swiss Federal Institute of Aquatic Science and Technology

²Institute of Biogeochemistry and Pollutant Dynamics (IBP), ETH Zürich

³Department of Zoology, University of Delhi

*Corresponding author: hanspeter.kohler@eawag.ch
phone +41 58 765 55 21, fax +41 58 765 50 28

19 Pages, 6 Figures, 6 Tables

Contents

S1 Materials	3
S1.1 Chemicals	3
S1.2 Stock solutions	3
S1.3 Synthesis of γ -pentachlorocyclohexene (γ -PCCH)	3
S1.4 Isotopic standards	4
S2 Protein expression and purification	4
S3 Conformational analysis	6
S4 Data evaluation	6
S4.1 Sequential dehydrochlorination kinetics	6
S4.2 Derivation of apparent kinetic isotope effects	8
S4.2.1 Dehydrochlorination of γ -HCH by LinA1	8
S4.2.2 Dehydrochlorination of γ -HCH by LinA2	11
S4.3 Kinetic isotope effects from isotopomer-specific concentration dynamics	11
S4.3.1 ^{13}C kinetic isotope effects	12
S4.3.2 ^2H kinetic isotope effects	13
S4.3.3 Sequential Dehydrochlorination Reactions	14
S4.3.4 Weighted averages of ^{13}C -AKIEs	16
S5 Dehydrochlorination sequences of γ-pentachlorocyclohexenes by LinA1	17
S6 Dehydrochlorination sequences of γ-pentachlorocyclohexenes by LinA2	18
S7 References	19

S1 Materials

S1.1 Chemicals

1,2,3-Trichlorobenzene (1,2,3-TCB, purity of 99.9 %) and 1,2,4-TCB (99.4 %), sodium hydroxide, hydrochloric acid, LB broth, L-(+)-arabinose, chloramphenicol, sodium chloride, Trizma®-base, glycine, imidazole, ethanol, aluminum sulfate hexadecahydrate, coomassie brilliant blue G250 and ortho-phosphoric acid (85%) were purchased from Fluka / Sigma-Aldrich. Sodium dihydrogen phosphate monohydrate, acetone, acetonitrile, *n*-hexane, ethyl acetate and patinal chromium powder from Merck. γ -Hexachlorocyclohexane (γ -HCH, 99 %) was purchased from Maag. Ampicillin sodium salt was obtained from AppliChem. Hexachlorobenzene was purchased from Santa Cruz Biotechnology. Diethylether was purchased from Riedel-de Haën.

S1.2 Stock solutions

Buffer solutions for fast-protein liquid chromatography (FPLC) and experiments were prepared with nanopure water (18.2 M Ω ·cm, Barnsted™ NANOpure™, Thermo Fisher Scientific) and the pH was adjusted with 5 or 0.5 mM sodium hydroxide (Sigma-Aldrich) or 1 mM hydrochloric acid (Fluka). All chemicals for buffers and microbiological work were used as received. For sodium dodecyl sulfate-polyacrylamide gel electrophoresis (SDS-PAGE) Novex®tricine SDS sample buffer (2x), invitrogen NuPAGE®reducing agent (10x) and was run with Novex®tricine SDS running buffer (all Thermo Fisher Scientific). Staining and destaining solutions were prepared according to Dyballa and Metzger⁴. We used precision plus protein™ Dual Color standard (Biorad), SeeBlue™ pre-stained protein standard (Thermo Fisher Scientific) or peqGold protein marker II (peqlab now part of VWR) as a protein standard.

S1.3 Synthesis of γ -pentachlorocyclohexene (γ -PCCH)

For the synthesis of γ -PCCH we incubated 500 mg of γ -HCH in 50 mL acetonitrile in a water bath at 40 °C. Dechlorination was started by the addition of 25 mL of 0.1 M NaOH (resulting pH > 12). After 20 minutes, we stopped the reaction by adding 5 mL of 32 % HCl (resulting pH = 1). γ -HCH, trichlorobenzenes (TCBs) and γ -PCCH were extracted twice with 20 mL of *n*-hexane. *n*-Hexane containing the extraction products was evaporated to a volume of 2 mL and loaded onto a silica gel column (silica gel 60, 230-400 mesh; 25 cm \times 2 cm i.d. glass column) with *n*-hexane as the eluent. Substances eluted successively from the column by washing the column with three eluents of different *n*-hexane:diethylether mixtures subsequently. The column was washed with 120 mL of each eluent. The diethyl ether concentration in the 120 mL portions of the eluents increased from 0% to 2.5% to 5% in the first, second, and third eluent solution. We collected fractions of 10 mL and analyzed them with a GC/MS. The fractions with the highest amounts of γ -PCCH and least amounts of other compounds were pooled and dried under a constant N₂ stream. Purity and structural identity of the obtained crystals were confirmed by means of nuclear magnetic resonance according to Bala et al.².

S1.4 Isotopic standards

Standard materials for C isotope analysis included γ -HCH ($\delta^{13}\text{C} = -26.7 \pm 0.1\text{‰}$), hexachlorobenzene standard 1 ($\delta^{13}\text{C} = -25.37 \pm 0.06\text{‰}$), and hexachlorobenzene standard 2 ($\delta^{13}\text{C} = -28.67 \pm 0.06\text{‰}$). For H isotope analysis, we used hexadecane ($\delta^2\text{H} = -9.1 \pm 1.4\text{‰}$) and heptadecane ($\delta^2\text{H} = -117.9 \pm 2.3\text{‰}$) and both materials were purchased from Schimmelmann et al.⁹, Indiana University.

S2 Protein expression and purification

Cells were grown in LB at 37 °C with an antibiotic pressure of 405 μM ampicillin and 105 μM chloramphenicol. At an OD_{600} of ≈ 0.6 , 2 g/L L-(+)-arabinose was added to induce the expression of the target enzyme, and the temperature was reduced to 30 °C. When the induced culture reached an OD_{600} of > 1.8 , we harvested the cells by centrifugation (10'000 rpm for 20 min at 4 °C) and stored the resulting pellets at -20 °C.

The protein purification was initiated by suspending 1 g of pelleted cells in 3 to 5 mL buffer (50 mM $\text{NaH}_2\text{PO}_4 \cdot \text{H}_2\text{O}$, 300 mM NaCl, 10 mM imidazole). Proteins were obtained after disrupting the cells by ultrasonication under constant cooling on ice using an ultrasonic homogeniser (Sonoplus HD 3200, Bandelin electronic) with an MS 73 needle at 65 % amplitude. The cells were sonicated with pulses (0.3 seconds pulse on; 0.5 seconds pulse off) for one minute. The procedure was repeated 5 times with intermissions of five minutes between runs to avoid heating of the cell extract. We purified LinA1 and LinA2 on two separate Ni-NTA Superflow cartridges (5 mL, Qiagen) with an ÄKTA FPLC system (GE Healthcare Life Science) to avoid cross-contamination. LinA1 and LinA2 proteins were eluted with an imidazole gradient from 10 mM to 300 mM. The concentration of proteins was quantified spectrophotometrically with a NanoDrop ND-1000 device (Thermo Scientific) at a wavelength of 280 nm as shown elsewhere.² The purity of the proteins was $> 95\%$ (Figures S1 and S2) as determined with an SDS-PAGE assay with Novex 10% Tricine gels (Invitrogen) and Coomassie Brilliant Blue staining enhanced with aluminum sulfate^{4,7}.

We prepared the staining solutions for SDS-Page gels according to Dyballa and Metzger⁴ but changed the staining protocol. The SDS-Page gels (Figures S1 and S2) were shaken on a horizontal shaker in nanopure water for 10 minutes. After disposing of the water, we put the gel in the staining solution and let it shake overnight. After removing the staining solution, we washed the gel in nanopure water and then soaked it in destaining solution on a shaker for 2 hours. Activity assays of the different purification steps of LinA1 and LinA2 were performed in tris-glycine buffer at pH 7.5 (200 mM glycine, 25 mM Trizma[®] base, final concentration) and 25 μM γ -HCH in a total reaction volume of 5 mL. After 0, 8, 16 and 32 minutes and 0, 1, 2 and 4 minutes for LinA1 and LinA2, respectively, the reactions were stopped with the addition of 2.5 mL ethyl acetate and the extracts analyzed by GC/MS. Both enzymes were purified several times with very similar outcome. The purification procedure results in total protein yields of 0.12 mg LinA1 and 0.029 mg LinA2 with specific activities of $6.2 \cdot 10^{-2}$ U/mg for LinA1 and

57 U/mg for LinA2.

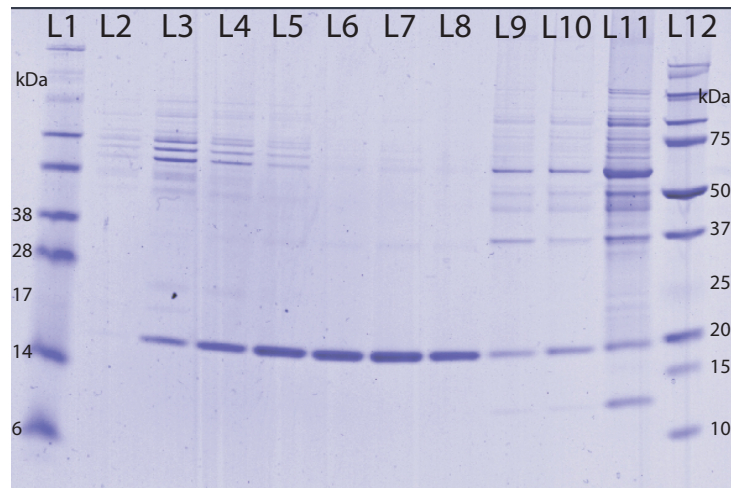


Figure S1 SDS-Page gel of purification of LinA1. L5-F8 were used in experiments. Lanes (left to right): L1, ladder (SeeBlue protein standard); L2-L8, collected fractions of FPLC; L9, unbinding proteins in FPLC; L10, cell extract; L11, cell lysate; L12, ladder (Precision plus protein standard).

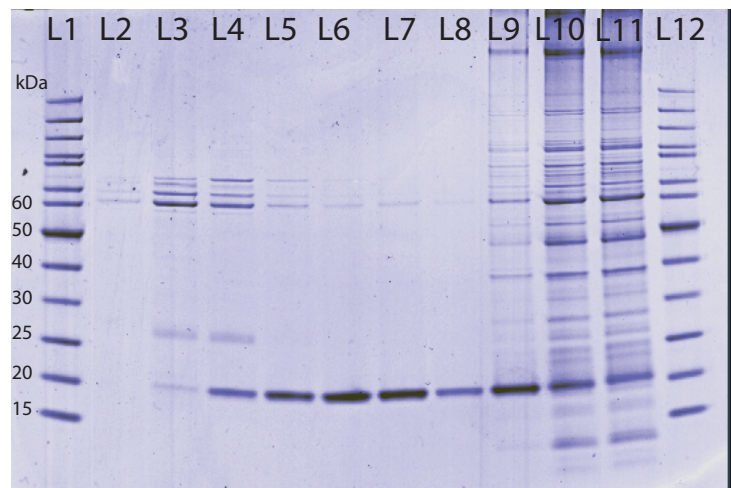


Figure S2 SDS-Page gel of purification of LinA2. L5-F8 were used in experiments. Lanes (left to right): L1, ladder (peqGOLD protein standard); L2-L8, collected fractions of FPLC; L9, unbinding proteins in FPLC; L10, cell extract; L11, cell lysate; L12, ladder.

S3 Conformational analysis

Data for calculating the abundance of two chair conformer of γ -HCH as well as of the two most stable conformers of the two γ -PCCH enantiomers are shown in Table S1. The free energy difference at standard conditions between the conformer 1 (Cf1) and the flipped conformer 2 (Cf2), $\Delta\Delta G^\circ$, was calculated with Marvin Beans (version 6.2, 2014 ChemAxon, <http://chemaxon.com>)

$$\Delta\Delta G^\circ = \Delta G_{\text{Cf2}}^\circ - \Delta G_{\text{Cf1}}^\circ = -RT \ln K \quad (\text{S1})$$

$$K = \frac{\text{Cf1}}{\text{Cf2}} \quad (\text{S2})$$

where $\Delta\Delta G^\circ$ is the difference between the standard free energies of the two conformers, $\Delta G_{\text{Cf2}}^\circ$ and $\Delta G_{\text{Cf1}}^\circ$, respectively, R is the gas constant, T is the absolute temperature, and K is the equilibrium constant for the population of the two conformers. To illustrate the time scales of changes of conformational mobility, we derived the frequency of conformational change, f_{flip} with eq. S3 and the results are shown in Table S1.

$$f_{\text{flip}} = \frac{k_{\text{B}}T}{h} e^{(-\Delta G^\ddagger/RT)} \quad (\text{S3})$$

S4 Data evaluation

S4.1 Sequential dehydrochlorination kinetics

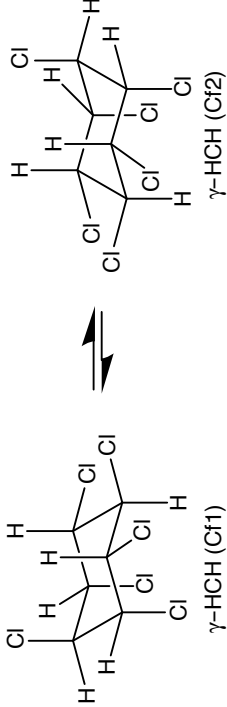
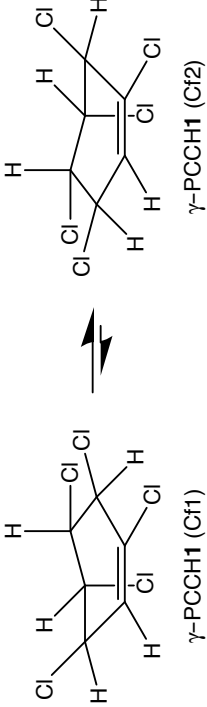
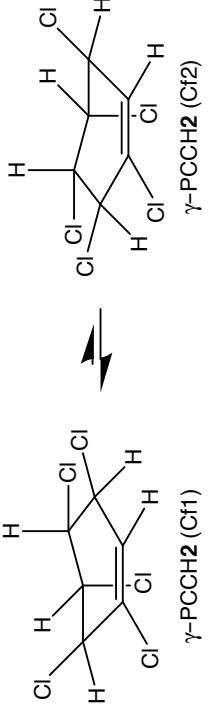
The sequential transformation of γ -HCH to PCCH enantiomers and TCB isomers according to Scheme 1 of the manuscript was implemented in Copasi⁶ to solve an array of ordinary differential equations (eq. S4).

$$\frac{dc_k}{dt} = \nu_i \cdot k_j \cdot c_k \quad (\text{S4})$$

where c_k is the chlorohydrocarbon species (γ -HCH, γ -PCCH enantiomers, trichlorobenzene isomers), k_j is the pseudo-first-order rate constant of decay and formation, and ν_i is the stoichiometric coefficient. k_j of the substrates γ -HCH and γ -PCCH are denoted as $k_{\text{obs},S}$ in eq. 1 of the manuscript.

Uncertainties of reaction rate constants reflect the parameter uncertainties from fitting the γ -HCH, γ -PCCH, and TCB concentration dynamics of one experiment to a series of first-order rate constants for sequential dehydrochlorination reactions. The uncertainty of the catalytic efficiencies $k_{\text{cat}}/K_{\text{m}}$ includes the propagated uncertainty of the measurement of initial enzyme concentrations (3 %). Because all experiments were carried out in duplicates, no meaningful averages can be derived to quantify the biological variability of different catalytic activities of enzyme purified in different batches. Instead, we present the derived parameters from two

Table S1 Relative free energies ($\Delta\Delta G^\circ$) of the two most stable conformers of γ -HCH, γ -PCCH1, and γ -PCCH2, equilibrium ration of conformers $K = \text{Cf1/Cf2}$, activation energy of their interconversion (ΔG^\ddagger), and frequency of conformational change, f_{flip} .

Substance	$\Delta\Delta G^\circ$ (kJ/mol)	Cf1/Cf2 ^b (-)	ΔG^\ddagger (kJ/mol)	f_{flip} (s ⁻¹)	Conformer
γ -HCH	0	1/1	40	$6.1 \cdot 10^6$	 γ -HCH (Cf1) γ -HCH (Cf2)
γ -PCCH1	4 ^a	1/5	21 ^c	$1.3 \cdot 10^9$	 γ -PCCH1 (Cf1) γ -PCCH1 (Cf2)
γ -PCCH2	-4 ^a	5/1	21 ^c	$1.3 \cdot 10^9$	 γ -PCCH2 (Cf1) γ -PCCH2 (Cf2)

^a Values for γ -PCCH calculated with Marvin Beans (version 6.2, 2014 ChemAxon, <http://chemaxon.com>);

^b relative abundance of the Cf1 and Cf2 at 298K from eq. S2;

^c Values from Anet and Haq¹ for ring inversion of chlorocyclohexene.

experiments separately in Tables S2 and S3.

S4.2 Derivation of apparent kinetic isotope effects

The calculation of apparent kinetic isotope effects, AKIE, for the dehydrochlorination of γ -HCH is based on the assignment of reactive atoms in the molecule.⁵ Due to the simultaneous presence of two γ -HCH conformers and different reactivities of LinA1 and LinA2 with those conformers, the assignment of reactive positions in γ -HCH requires detailed discussion.

As shown in Figure S3, γ -HCH exhibits two superimposable conformers **Cf1** and **Cf2**. However, their equatorial and axial relationships of atoms are different. In general, γ -HCH dehydrochlorination only occurs when H and Cl atoms in H–C–C–Cl moieties align in *trans*-diaxial position. Both conformers exhibit two such reactive positions which include atoms H₉–C₃–C₂–Cl and H₁₁–C₅–C₆–Cl in conformer Cf1 and atoms H₈–C₂–C₃–Cl and H₁₂–C₆–C₅–Cl in conformer Cf2. The numbering of atoms for the identification of reactive positions is shown in the bottom row of Figure S3.

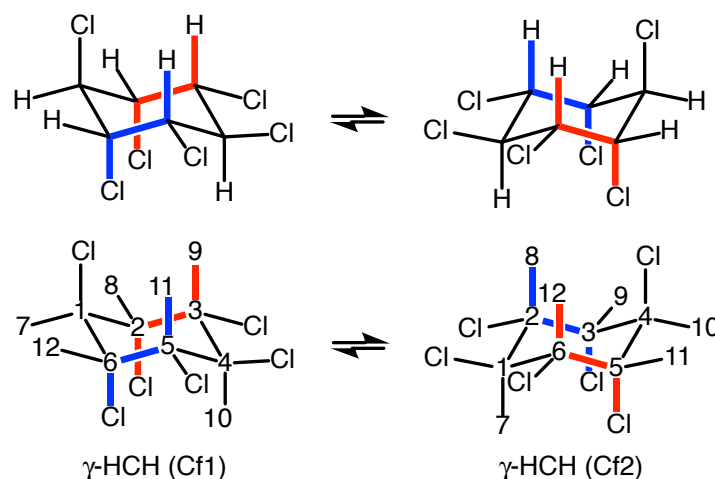


Figure S3 γ -HCH conformers Cf1 and Cf2. Blue and red bonds indicate the two possible, *trans*-diaxial arrangements of reactive H–C–C–Cl bonds for dehydrochlorination. Whereas LinA1 reacts with both (red and blue) H–C–C–Cl arrangements, LinA2 only dehydrochlorinates the blue arrangement. Bottom row shows both conformers with numbered carbon (1-6) and hydrogen (7-12) atoms.

S4.2.1 Dehydrochlorination of γ -HCH by LinA1

Dehydrochlorinations of γ -HCH by LinA1 can occur at two reactive H–C–C–Cl moieties in each conformer, that is H₉–C₃–C₂–Cl and H₁₁–C₅–C₆–Cl in conformer **Cf1** and atoms H₈–C₂–C₃–Cl and H₁₂–C₆–C₅–Cl in conformer **Cf2**. For the calculation of apparent ¹³C kinetic isotope effects in a bimolecular elimination (E2) mechanism, 4 of 6 C atoms (C₂, C₃, C₅, C₆) in the molecule were located at reactive positions ($x = 4$). Because of the concerted E2 mechanisms 2 of 4 reactive C atoms were in intramolecular isotopic competition ($z = 2$). The

Table S2 First order reaction rate constants k_j obtained from fitting eq. S4 in Copasi and catalytic efficiencies, k_{cat}/K_m , from individual experiments. Initial LinA1 concentrations in experiments 1 and 2 were $4.9 \pm 0.1 \mu\text{g/mL}$ and $4.1 \pm 0.1 \mu\text{g/mL}$, respectively. Initial LinA2 concentrations in experiments 1 and 2 were $0.93 \pm 0.03 \mu\text{g/mL}$ and $0.51 \pm 0.02 \mu\text{g/mL}$, respectively.^a

Reaction step	k_j (s^{-1}) ^a		k_{cat}/K_m ($\text{M}^{-1}\text{s}^{-1}$)	
	Exp. 1	Exp. 2	Exp. 1	Exp. 2
LinA1				
$\gamma\text{-HCH} \rightarrow \gamma\text{-PCCCH1}$	$(2.8 \pm 0.1) \cdot 10^{-5}$	$(1.3 \pm 0.3) \cdot 10^{-5}$	100 ± 0.1	52 ± 0.4
$\gamma\text{-HCH} \rightarrow \gamma\text{-PCCCH2}$	$(1.0 \pm 0.1) \cdot 10^{-4}$	$(6.1 \pm 1.3) \cdot 10^{-5}$	360 ± 0.3	250 ± 2
$\gamma\text{-PCCCH1} \rightarrow 1,2,3\text{-TCB}$	$(2.2 \pm 0.1) \cdot 10^{-5}$	$(9.4 \pm 4.8) \cdot 10^{-6}$	76 ± 0.1	38 ± 0.6
$\gamma\text{-PCCCH1} \rightarrow 1,2,4\text{-TCB}$	$(1.8 \pm 0.1) \cdot 10^{-5}$	$(1.4 \pm 0.1) \cdot 10^{-5}$	65 ± 0.2	56 ± 1.2
$\gamma\text{-PCCCH2} \rightarrow 1,2,3\text{-TCB}$	n.d. ^b	n.d.	n.d.	n.d.
$\gamma\text{-PCCCH2} \rightarrow 1,2,4\text{-TCB}$	$(1.9 \pm 0.1) \cdot 10^{-3}$	$(1.2 \pm 0.23) \cdot 10^{-3}$	6700 ± 6	4800 ± 28
LinA2				
$\gamma\text{-HCH} \rightarrow \gamma\text{-PCCCH1}$	$(9.1 \pm 0.2) \cdot 10^{-4}$	$(1.0 \pm 0.1) \cdot 10^{-4}$	$(1.7 \pm 0.1) \cdot 10^4$	$(3.4 \pm 0.1) \cdot 10^3$
$\gamma\text{-PCCCH1} \rightarrow 1,2,4\text{-TCB}$	$(1.6 \pm 0.1) \cdot 10^{-3}$	$(2.4 \pm 0.2) \cdot 10^{-4}$	$(2.9 \pm 0.1) \cdot 10^4$	$(8.3 \pm 0.1) \cdot 10^3$

^a Uncertainties below $< 0.1 \cdot 10^{-x} \text{ s}^{-1}$ or $< 0.1 \cdot 10^{-x} \text{ M}^{-1}\text{s}^{-1}$, where x is the order of magnitude of the entry, are not shown for simplicity; ^b “n.d.” = not detected.

Table S3 First order reaction rate constants k_j obtained from fitting eq. S4 in Copasi and catalytic efficiencies k_{cat}/K_m from individual experiments with γ -PCCH as substrate. Experiment with LinA1 was only done once. Initial LinA1 and LinA2 concentrations were $40 \pm 1 \text{ } \mu\text{g/mL}$ and $0.60 \pm 0.02 \text{ } \mu\text{g/mL}$, respectively.^a

Reaction step	$k_j \text{ (s}^{-1}\text{)}^a$		$k_{\text{cat}}/K_m \text{ (M}^{-1}\text{s}^{-1}\text{)}$	
	Exp. 1	Exp. 2	Exp. 1	Exp. 2
LinA1				
γ -PCCH1 \rightarrow 1,2,3-TCB	$(1.6 \pm 0.1) \cdot 10^{-4}$	n.a. ^b	$(1.5 \pm 0.1) \cdot 10^2$	n.a.
γ -PCCH1 \rightarrow 1,2,4-TCB	$(1.1 \pm 0.1) \cdot 10^{-4}$	n.a.	$(9.5 \pm 0.1) \cdot 10^1$	n.a.
γ -PCCH2 \rightarrow 1,2,3-TCB	$(1.5 \pm 0.1) \cdot 10^{-4}$	n.a.	$(1.4 \pm 0.1) \cdot 10^2$	n.a.
γ -PCCH2 \rightarrow 1,2,4-TCB	$(1.1 \pm 0.1) \cdot 10^{-2}$	n.a.	$(1.0 \pm 0.1) \cdot 10^4$	n.a.
LinA2				
γ -PCCH1 \rightarrow 1,2,4-TCB	$(9.7 \pm 0.3) \cdot 10^{-3}$	$(5.6 \pm 0.2) \cdot 10^{-3}$	$(2.7 \pm 0.1) \cdot 10^2$	$(1.7 \pm 0.3) \cdot 10^2$
γ -PCCH2 \rightarrow 1,2,3-TCB	$(2.4 \pm 0.1) \cdot 10^{-3}$	$(1.1 \pm 0.1) \cdot 10^{-3}$	$(6.7 \pm 0.2) \cdot 10^1$	$(3.2 \pm 0.2) \cdot 10^1$

^a Uncertainties below $< 0.1 \cdot 10^{-x} \text{ s}^{-1}$, where x is the order of magnitude of the entry, are not shown for simplicity;

^b “n.a.” = not applicable.

correction factor $n/x \cdot z$ in eq. 3 of the manuscript for the dehydrochlorination of γ -HCH by LinA1 was thus $6/4 \cdot 2 = 3$.

S4.2.2 Dehydrochlorination of γ -HCH by LinA2

By contrast, when γ -HCH is bound by LinA2, only one of the two H–C–C–Cl *trans*-diaxial moieties in each conformer was found to be reactive^{8,10}. The reactive position for dehydrochlorination of γ -HCH conformer **Cf1** by LinA2 is shown in blue in Figure S3 implying that dehydrochlorination happens from the H₁₁–C₅–C₆–Cl moiety. Due to different equatorial and axial relationships of the H and Cl atoms in **Cf2**, its H₁₂–C₆–C₅–Cl moiety was no longer reactive with LinA2. Instead, dehydrochlorination from Cf2 happens from the H₈–C₂–C₃–Cl moiety. γ -HCH bound by LinA2 thus exhibited 4 C atoms from which a dehydrochlorination could occur. Even though γ -HCH conformers Cf1 and Cf2 can interconvert through ring flipping, LinA2 will never encounter γ -HCH molecules in which all 4 reactive C atom (C₂–C₃ vs C₄–C₅) were equally susceptible for dehydrochlorination. Because both conformers have equal thermodynamic stability (see Section S3), and therefore Cf1 and Cf2 were equally abundant, only 2 of the 4 potentially reactive C atoms could undergo a dehydrochlorination. The number of reactive C atoms, x , in a mixture of two conformers, therefore, equals 2. Due to the concerted E2 dehydrochlorination mechanism, both C are equally reactive, and intramolecular isotopic competition was absent ($z = 1$). The correction factor $n/x \cdot z$ for the dehydrochlorination of γ -HCH by LinA2 was thus $6/2 \cdot 1 = 3$ and equal to the one for the reaction with LinA1.

S4.3 Kinetic isotope effects from isotopomer-specific concentration dynamics

We quantified the ¹³C and ²H kinetic isotope effects pertinent to the dehydrochlorination of γ -HCH with an isotopomer-specific model shown in eq S5 based on the assignment of reactive C and H atoms made above in Section S4.2.

$$\frac{dc_i^E}{dt} = \sum_j \nu_i \cdot \omega_i^E \cdot k_j^E \cdot c_i^E \quad (\text{S5})$$

where c_i^E is the concentration of a γ -HCH isotopomer i of element E, ν_i is the stoichiometric coefficient indicating decay or formation of an isotopomer, ω_i^E is the probability of isotopomer i to have a heavy or light isotope at the reactive position, and k_j^E is the pseudo-first-order rate constant for reaction of an isotopomer according to the presence of the light (l) or heavy (h) isotope at the reactive position (k_l^E and k_h^E). The model assumptions and parameter values used for taking into account the different reactivity of γ -HCH conformers (Figure S3) with LinA1 and LinA2 are illustrated here.

S4.3.1 ^{13}C kinetic isotope effects

Calculation of ^{13}C -KIEs was based on the explicit consideration of 7 C isotopomers containing either exclusively ^{12}C (isotopomer HCH-*l*) or one ^{13}C atom in positions C₁ to C₆ (isotopomers HCH-*h1* to HCH-*h6*) as shown in Table S4.

- The ^{12}C -isotopomer HCH-*l* would always react with the rate constant for light C isotopes, k_l^{C} , and consequently, the probability that a light C atom was at the reactive position, $\omega^{12\text{C}}$, equals 1 and the probability that a heavy C atom was at the reactive position, $\omega^{13\text{C}}$, equals 0. Likewise, all ^{13}C -isotopomers with ^{13}C in the non-reactive positions, C₁ (HCH-*h1*) and C₄ (HCH-*h4*), would react with k_l^{C} so that $\omega^{12\text{C}}$ equals 1 and $\omega^{13\text{C}}$ equals 0. This interpretation was valid for both γ -HCH conformers in reactions catalyzed by LinA1 and LinA2.
- ^{13}C -Isotopomers with ^{13}C in the reactive positions C₂ (HCH-*h2*), C₃ (HCH-*h3*), C₅ (HCH-*h5*) and C₆ (HCH-*h6*) reacted with either one of the rate constants for light and heavy C atoms, k_l^{C} and k_h^{C} , respectively. Isotopomer HCH-*h5* was arbitrarily selected as an example here to illustrate the reactivity of its conformers with LinA1 and LinA2. The transformation of **conformer Cf1** of isotopomer **HCH-*h5*** catalyzed by **LinA1** could occur at H₉–C₃–C₂–Cl and H₁₁–C₅–C₆–Cl (Figure S3). In 50% of all cases, HCH-*h5* was transformed through a reaction at H₉–C₃–C₂–Cl where no ^{13}C substitution exists. The probability of this reaction with rate constant k_l^{C} was captured by setting $\omega^{12\text{C}}$ to 0.5. However, in the other 50%, HCH-*h5* was transformed through a reaction at H₁₁–C₅–C₆–Cl where there was indeed ^{13}C substitution at the C₅ position. As a consequence, the probability of this reaction with rate constant k_h^{C} to happen was 50% so that $\omega^{13\text{C}}$ also amounted to 0.5 (Table S4).
- The same reasoning could be applied to the transformation of **conformer Cf2** of isotopomer **HCH-*h5*** by **LinA1** and the resulting $\omega_i^{13\text{C}}$ -values for Cf2 were identical to those for Cf1. Therefore, no distinction of γ -HCH conformers was necessary to derive the ^{13}C -AKIE for the dehydrochlorination of γ -HCH by LinA1 with eq. S5.
- The transformation of **conformer Cf1** of isotopomer **HCH-*h5*** by **LinA2** could be illustrated by assuming that one *trans*-diaxial arrangement (e.g., H₁₁–C₅–C₆–Cl) was reactive as discussed above in Section S4.2 (blue bonds highlighted in Figure S3). With this assumption, the $\omega_i^{13\text{C}}$ -value for reaction of Cf1 of isotopomer HCH-*h5* equals 1. Conversely, the transformation of **conformer Cf2** of isotopomer **HCH-*h5*** by **LinA2** does not take place at H₁₂–C₆–C₅–Cl. Only the H₈–C₂–C₃–Cl moiety of Cf2 was reactive. However, because there was no ^{13}C substitution in this moiety of Cf2 of isotopomer HCH-*h5*, the $\omega_i^{13\text{C}}$ -value equals 0. The equal abundance of both γ -HCH conformers during their reaction with LinA2 therefore results in an averaging of $\omega_i^{13\text{C}}$ and $\omega_i^{12\text{C}}$ -values to 0.5
- From the $\omega^{12\text{C}}$ and $\omega^{13\text{C}}$ values shown in Table S4 it became apparent that even though the two conformers of γ -HCH exhibit different reactivity with LinA1 and LinA2, they

contribute to the observable C isotope fractionation in a mathematically identical way.

Table S4 Carbon isotopomers considered for the isotopomer-specific analysis of C isotope fractionation associated with the dehydrochlorination of γ -HCH by LinA1 and LinA2.

Isotopomer	Position of isotopic substitution						LinA1		LinA2	
	C ₁	C ₂	C ₃	C ₄	C ₅	C ₆	$\omega^{12\text{C}}$	$\omega^{13\text{C}}$	$\omega^{12\text{C}}$	$\omega^{13\text{C}}$
HCH- <i>l</i>	¹² C	¹² C	¹² C	¹² C	¹² C	¹² C	1	0	1	0
HCH- <i>h1</i>	¹³ C	¹² C	¹² C	¹² C	¹² C	¹² C	1	0	1	0
HCH- <i>h2</i>	¹² C	¹³ C	¹² C	¹² C	¹² C	¹² C	0.5	0.5	0.5	0.5
HCH- <i>h3</i>	¹² C	¹² C	¹³ C	¹² C	¹² C	¹² C	0.5	0.5	0.5	0.5
HCH- <i>h4</i>	¹² C	¹² C	¹² C	¹³ C	¹² C	¹² C	1	0	1	0
HCH- <i>h5</i>	¹² C	¹² C	¹² C	¹² C	¹³ C	¹² C	0.5	0.5	0.5	0.5
HCH- <i>h6</i>	¹² C	¹² C	¹² C	¹² C	¹² C	¹³ C	0.5	0.5	0.5	0.5

S4.3.2 ²H kinetic isotope effects

Calculation of ²H-KIEs was based on the explicit consideration of 7 H isotopomers containing either exclusively ¹H (isotopomer HCH-*l*) or one ²H atom in positions H₇ to H₁₂ (isotopomers HCH-*h7* to HCH-*h12*) as shown in Table S5. Procedures for accounting for conformational mobility as well as different reactivities of the two LinA variants follow from the above considerations for calculation of ¹³C-AKIEs (Section S4.3.1).

- The ¹H-isotopomer HCH-*l* would always react with the rate constant for light H isotopes, k_l^{H} , and consequently, $\omega^{1\text{H}}$ equals 1 and $\omega^{2\text{H}}$ equals 0. Likewise, all ²H-isotopomers with ²H in the non-reactive positions, that was H₇ (HCH-*h7*) and H₁₀ (HCH-*h10*) in **LinA1**, and H₇ (HCH-*h7*), H₉ (HCH-*h9*), H₁₀ (HCH-*h10*) and H₁₂ (HCH-*h12*) in **LinA2** would react with k_l^{H} so that $\omega^{1\text{H}}$ equals 1 whereas $\omega^{2\text{H}}$ equals 0. This interpretation was valid for both γ -HCH conformers in reactions with LinA1 and LinA2.
- ²H-Isotopomers with ²H in the reactive positions H₈ (HCH-*h8*), H₉ (HCH-*h9*), H₁₁ (HCH-*h11*), and H₁₂ (HCH-*h12*) reacted with either one of the rate constants for light and heavy H atoms, k_l^{H} and k_h^{H} , respectively. The transformation of **conformer Cf1** of isotopomer **HCH-*h11*** by **LinA1** could occur at H₉–C₃–C₂–Cl and H₁₁–C₅–C₆–Cl (Figure S3). In 50% of all cases, HCH-*h11* was transformed through a reaction at H₁₁–C₅–C₆–Cl where ²H substitution does exist. The probability of this reaction with rate constant k_h^{H} was captured by setting $\omega^{2\text{H}}$ to 0.5. However, in the other 50%, HCH-*h11* was transformed through a reaction at H₉–C₃–C₂–Cl where there was no ²H substitution at the H₉ position. As a consequence, the probability of the transformation of **conformer Cf1** with rate constant k_l^{H} to happen was 50%. Conversely, the transformation of **conformer Cf2** of isotopomer **HCH-*h11*** by **LinA1** could occur at H₈–C₂–C₃–Cl and H₁₂–C₆–C₅–Cl

(Figure S3). Because no ^2H was present in any of those reactive positions, conformer Cf2 of isotopomer HCH-*h*11 would react with the rate constant k_l^{H} . The $\omega^{1\text{H}}$ and $\omega^{2\text{H}}$ values in Table S5 reflect the average of two HCH-*h*11 conformers. In 3 of 4 possible dehydrochlorination scenarios (reactions at $\text{H}_9\text{--C}_3\text{--C}_2\text{--Cl}$ and $\text{H}_{11}\text{--C}_5\text{--C}_6\text{--Cl}$ in Cf1 vs reactions at $\text{H}_8\text{--C}_2\text{--C}_3\text{--Cl}$ and $\text{H}_{12}\text{--C}_6\text{--C}_5\text{--Cl}$ in Cf2), the HCH-*h*11 conformers would transform with k_l^{H} and $\omega^{1\text{H}}$ amounts 0.75. Only in 1 scenario, would the dehydrochlorination of HCH-*h*11 happen with k_h^{H} so that $\omega^{2\text{H}}$ is 0.25.

- The same reasoning applies to dehydrochlorination of **conformers Cf1** and **Cf2** of isotopomers **HCH-*h*8**, **HCH-*h*9**, and **HCH-*h*12** by **LinA1** leading to identical $\omega^{1\text{H}}$ and $\omega^{2\text{H}}$ values in Table S5.
- For reactions catalyzed by **LinA2**, in addition to HCH-*h*7 and HCH-*h*10, the ^2H -isotopomers HCH-*h*9 and HCH-*h*12 also contain ^2H in non-reactive positions. Therefore, their $\omega^{1\text{H}}$ and $\omega^{2\text{H}}$ values are all 1 and 0, respectively (Table S5).
- Only HCH-8 and HCH-*h*11 exhibit ^2H substitution at reactive positions. Whereas only the $\text{H}_{11}\text{--C}_5\text{--C}_6\text{--Cl}$ position of **Cf1** of **HCH-*h*11** was reactive in **LinA2**, there was a 100% probability that this isotopomer reacts with k_h^{H} . Conversely, **Cf2** of **HCH-*h*11** exclusively reacts with k_l^{H} . The conformer-averaged $\omega^{1\text{H}}$ and $\omega^{2\text{H}}$ values of **HCH-*h*11** are thus 0.5. The same logic applies for deriving $\omega^{1\text{H}}$ and $\omega^{2\text{H}}$ values of **HCH-*h*8** for reactions catalyzed by LinA2.

Table S5 Hydrogen isotopomers considered for the isotopomer-specific analysis of H isotope fractionation associated with the dehydrochlorination of γ -HCH by LinA1 and LinA2.

Isotopomer	Position of isotopic substitution						LinA1		LinA2	
	H ₇	H ₈	H ₉	H ₁₀	H ₁₁	H ₁₂	$\omega^{1\text{H}}$	$\omega^{2\text{H}}$	$\omega^{1\text{H}}$	$\omega^{2\text{H}}$
HCH- <i>l</i>	^1H	^1H	^1H	^1H	^1H	^1H	1	0	1	0
HCH- <i>h</i> 7	^2H	^1H	^1H	^1H	^1H	^1H	1	0	1	0
HCH- <i>h</i> 8	^1H	^2H	^1H	^1H	^1H	^1H	0.75	0.25	0.5	0.5
HCH- <i>h</i> 9	^1H	^1H	^2H	^1H	^1H	^1H	0.75	0.25	1	0
HCH- <i>h</i> 10	^1H	^1H	^1H	^2H	^1H	^1H	1	0	1	0
HCH- <i>h</i> 11	^1H	^1H	^1H	^1H	^2H	^1H	0.75	0.25	0.5	0.5
HCH- <i>h</i> 12	^1H	^1H	^1H	^1H	^1H	^2H	0.75	0.25	1	0

S4.3.3 Sequential Dehydrochlorination Reactions

Following the same procedures described above, we quantified the kinetic isotope effects of the dechlorination reactions leading from γ -PCCH isomers and enantiomers to selected TCB isomers. To this end, selected pentachlorocyclohexene and trichlorobenzene species shown in Figure S4 were included in eq S5. Results of the isotopomer specific modelling can be found in Table S6.

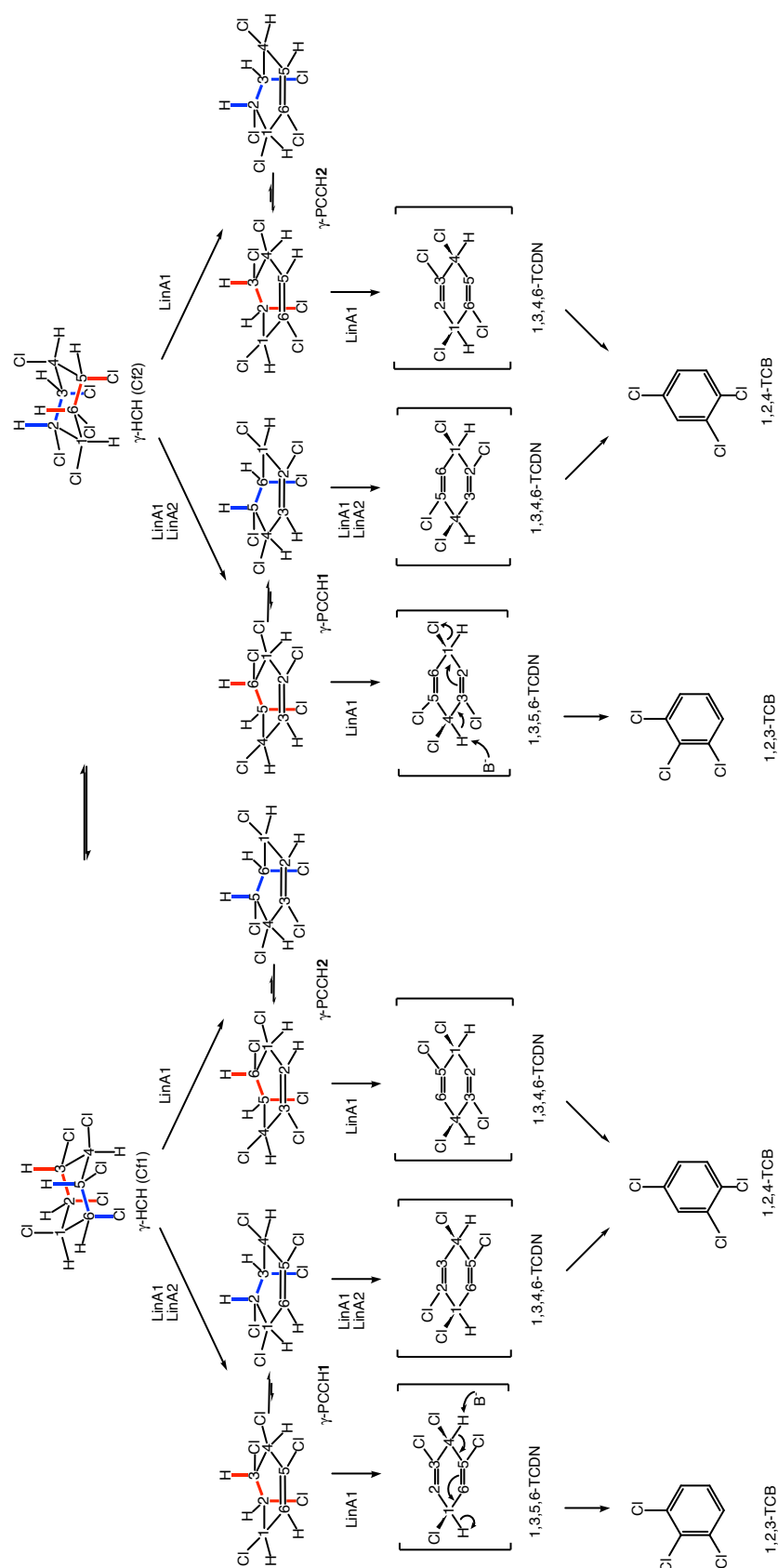


Figure S4 Dehydrochlorination sequences included in the isotopomer-specific numerical model for the derivation of kinetic isotope effects for the transformation of γ -HCH and γ -PCCH enantiomers and conformers to selected TCB isomers. The C atoms of γ -HCH, γ -PCCH, and TCDN are numbered for a distinction of reactive positions and isotopic substitution in the different conformers in analogy to Figure S3. The numbering does not represent IUPAC naming. The blue and red bonds highlight the different spatial arrangements of reactive H-C-Cl moieties in γ -HCH and γ -PCCH. Different γ -HCH conformers are labelled as (Cf1) and (Cf2).

Table S6 Carbon isotope enrichment factors as well as apparent ^{13}C and ^2H kinetic isotope effects (^{13}C -AKIE and ^2H -AKIE) derived for sequential dehydrochlorination reactions of γ -HCH with LinA enzymes with the isotopomer-specific model (eq S5).

Reaction	$\epsilon_{\text{C}}^{\text{a}}$ (‰)	^{13}C -AKIE (-)	^2H -AKIE (-)
LinA2			
$\gamma\text{-HCH} \rightarrow \gamma\text{-PCCH1}$	-8.7 ± 0.1	1.027 ± 0.0005	2.6 ± 0.1
$\gamma\text{-PCCH1} \rightarrow 1,2,4\text{-TCB}$	-6.9 ± 0.7	1.021 ± 0.002	- ^b
LinA1			
$\gamma\text{-HCH} \rightarrow \gamma\text{-PCCH}^{\text{c}}$	-8.4 ± 0.7	1.026 ± 0.002	2.4 ± 0.1
$\gamma\text{-PCCH} \rightarrow 1,2,3\text{-TCB}^{\text{c}}$	-11.2 ± 1.3	1.036 ± 0.004	- ^b
$\gamma\text{-PCCH} \rightarrow 1,2,4\text{-TCB}^{\text{c}}$	-7.5 ± 3.6	1.023 ± 0.011	- ^b

^a $\epsilon_{\text{C}} = (^{13}\text{C}\text{-AKIE}^{-1} - 1) / 3$; ^b - = not determined;

^c due to lack of enantiomer-specific data for $\gamma\text{-PCCH1}$ and $\gamma\text{-PCCH2}$, only one type of $\gamma\text{-PCCH}$ species was considered in the calculation.

S4.3.4 Weighted averages of ^{13}C -AKIEs

Weighted average calculations of ^{13}C AKIEs from the dehydrochlorination of $\gamma\text{-HCH}$ by LinA1 were carried out with eqs S6 to S8.

$$^{13}\text{C}\text{-AKIE}_{\text{red}} = \frac{^{13}\text{C}\text{-AKIE}_{\text{obs}} - ^{13}\text{C}\text{-AKIE}_{\text{blue}} \cdot \alpha_{\text{blue}}}{\alpha_{\text{red}}} \quad (\text{S6})$$

$$\alpha_{\text{blue}} = \frac{(k_{\text{cat}}/K_{\text{M}})_{\gamma\text{-HCH} \rightarrow \gamma\text{-PCCH1}}}{(k_{\text{cat}}/K_{\text{M}})_{\gamma\text{-HCH} \rightarrow \gamma\text{-PCCH1}} + (k_{\text{cat}}/K_{\text{M}})_{\gamma\text{-HCH} \rightarrow \gamma\text{-PCCH2}}} \quad (\text{S7})$$

$$\alpha_{\text{red}} = 1 - \alpha_{\text{blue}} \quad (\text{S8})$$

where “obs” refers to the AKIE-values derived with the isotopomer-specific model, eq. 4 in the main manuscript, “blue” and “red” denote dehydrochlorination of H–C–C–Cl moieties highlighted in blue and red, respectively, in Scheme 1 and Figure S3. α_{blue} and α_{red} are the branching ratios to $\gamma\text{-PCCH1}$ and $\gamma\text{-PCCH2}$, respectively.

S5 Dehydrochlorination sequences of γ -pentachlorocyclohexenes by LinA1

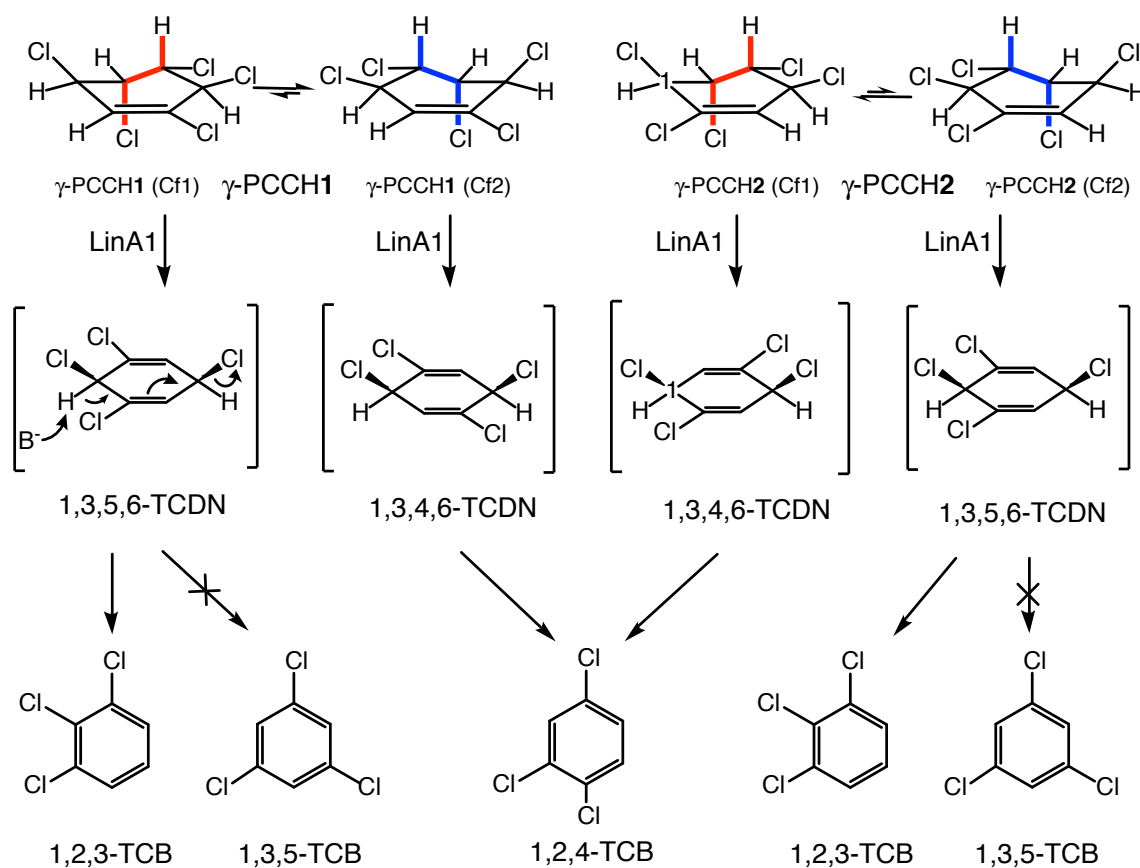


Figure S5 Dehydrochlorination of γ -PCCH enantiomers γ -PCCH1 and γ -PCCH2 by **LinA1**. Reactive H-C-C-Cl moieties are highlighted in red and blue color. The *anti*-1,4-elimination from TCDN intermediates to TCB is assumed to occur spontaneously. The concentration dynamics shown in Figure 1d imply that 1,2,4-TCB was formed predominantly from conformer Cf1 of γ -PCCH2. In contrast, 1,2,3-TCB originated from both γ -PCCH enantiomers. 1,3,5-TCB could have been formed theoretically from 1,3,5,6-TCN but was not observed in our experiments.

S6 Dehydrochlorination sequences of γ -pentachlorocyclohexenes by LinA2

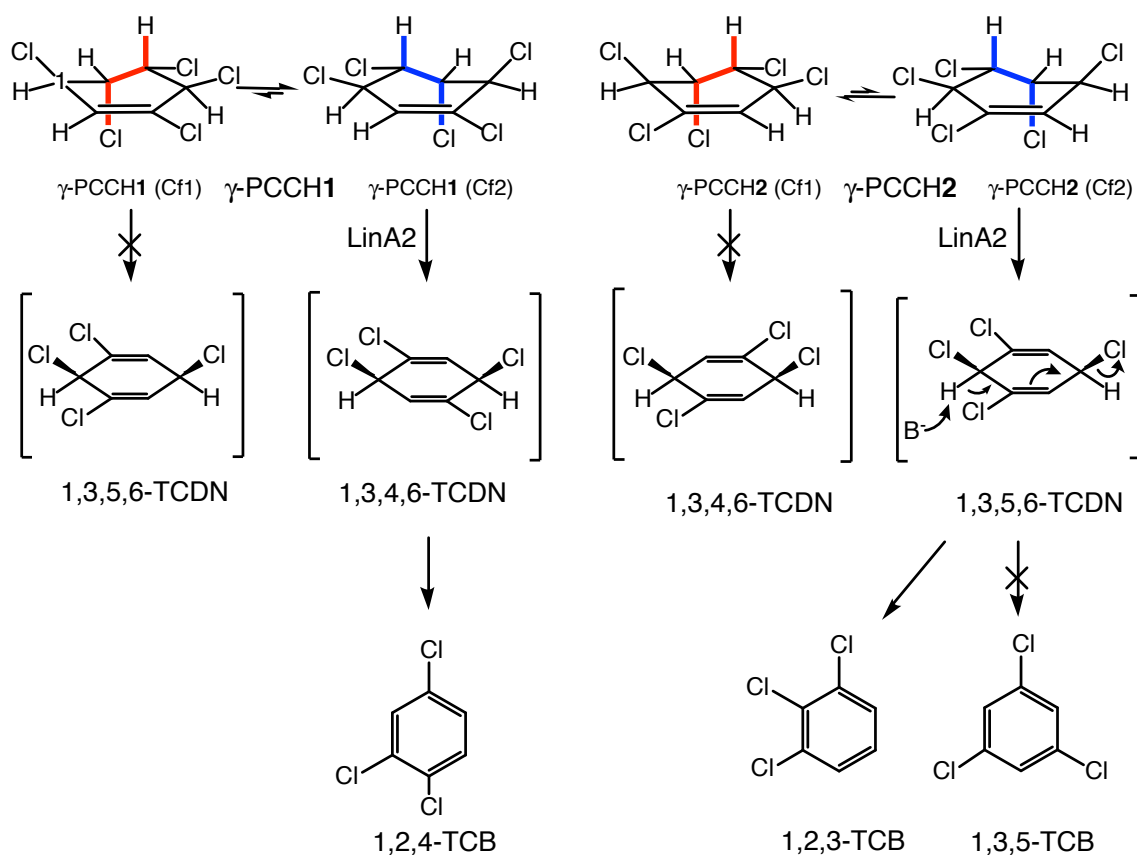


Figure S6 Dehydrochlorination of γ -PCCH enantiomers γ -PCCH1 and γ -PCCH2 by **LinA2**. Reactive H–C–C–Cl moieties are highlighted in red and blue color but only those highlighted in blue were transformed by LinA2. The *anti*-1,4-elimination from TCDN intermediates to TCB occur spontaneously. The concentration dynamics shown in Figure 1b imply that for 1,2,4-TCB was formed from γ -PCCH1. Consequently, 1,2,4-TCB could not have been formed from 1,3,4,6-TCDN that originates from dehydrochlorination of conformer Cf1 of γ -PCCH2. Therefore we conclude that conformer Cf1 of γ -PCCH2 does not react with LinA2 (crossed arrow). The same logic applies to the conformer-specific transformation of γ -PCCH2. The concentration dynamics shown in Figure 1b also imply that for 1,2,3-TCB was formed from γ -PCCH2. Consequently, 1,2,3-TCB could not have been formed from 1,3,5,6-TCDN that originates from dehydrochlorination of conformer Cf1 of γ -PCCH1. Therefore we conclude that conformer Cf1 of γ -PCCH1 does not react with LinA2 (crossed arrow). 1,3,5-TCB could have been formed theoretically from 1,3,5,6-TCN but was not observed in our experiments.

S7 References

- [1] Anet, F. A. L. and Haq, M. Z. (1965). Ring inversion in cyclohexene. *J. Am. Chem. Soc.*, 87(14):3147–3150.
- [2] Bala, K., Geueke, B., Miska, M. E., Rentsch, D., Poiger, T., Dadhwal, M., Lal, R., Holliger, C., and Kohler, H.-P. E. (2012). Enzymatic conversion of ϵ -hexachlorocyclohexane and a heptachlorocyclohexane isomer, two neglected components of technical hexachlorocyclohexane. *Environ. Sci. Technol.*, 46(7):4051–4058.
- [3] Burgess, R. R. (2009). Chapter 4 preparing a purification summary table. In Burgess, R. R. and Deutscher, M. P., editors, *Guide to Protein Purification, 2nd Edition*, volume 463 of *Methods in Enzymology*, pages 29–34. Academic Press.
- [4] Dyballa, N. and Metzger, S. (2009). Fast and sensitive colloidal coomassie G-250 staining for proteins in polyacrylamide gels. *J. Vis. Exp.*, (30).
- [5] Elsner, M., Zwank, L., Hunkeler, D., and Schwarzenbach, R. P. (2005). A new concept linking observable stable isotope fractionation to transformation pathways of organic pollutants. *Environ. Sci. Technol.*, 39(18):6896–6916.
- [6] Hoops, S., Sahle, S., Gauges, R., Lee, C., Pahle, J., Simus, N., Singhal, M., Xu, L., Mendes, P., and Kummer, U. (2006). COPASI - a complex pathway simulator. *Bioinformatics*, 22(24):3067–3074.
- [7] Kang, D., Gho, Y. S., Suh, M., and Kang, C. (2002). Highly sensitive and fast protein detection with coomassie brilliant blue in sodium dodecyl sulfate-polyacrylamide gel electrophoresis. *Bull. Korean Chem. Soc.*, 23(11):1511–1512.
- [8] Okai, M., Kubota, K., Fukuda, M., Nagata, Y., Nagata, K., and Tanokura, M. (2010). Crystal structure of γ -hexachlorocyclohexane dehydrochlorinase LinA from *Sphingobium japonicum* UT26. *J. Mol. Biol.*, 403(2):260–269.
- [9] Schimmelmann, A., Qi, H., Coplen, T. B., Brand, W. A., Fong, J., Meier-Augenstein, W., Kemp, H. F., Toman, B., Ackermann, A., Assonov, S., Aerts-Bijma, A. T., Brejcha, R., Chikaraishi, Y., Darwish, T., Elsner, M., Gehre, M., Geilmann, H., Gröning, M., Helie, J.-F., Herrero-Martín, S., Meijer, H. A. J., Sauer, P. E., Sessions, A. L., and Werner, R. A. (2016). Organic reference materials for hydrogen, carbon, and nitrogen stable isotope-ratio measurements: Caffeines, n-alkanes, fatty acid methyl esters, glycines, l-valines, polyethylenes, and oils. *Anal. Chem.*, 88(8):4294–4302.
- [10] Trantirek, L., Hynkova, K., Nagata, Y., Murzin, A., Ansorgova, A., Sklenar, V., and Damborsky, J. (2001). Reaction mechanism and stereochemistry of γ -hexachlorocyclohexane dehydrochlorinase LinA. *J. Biol. Chem.*, 276(11):7734–7740.